Fast Interactive Simulations of Mitral Valve Repair

Neil A. Tenenholtz, Peter E. Hammer, Robert D. Howe

***Keywords*: Surgical simulation, human-computer interaction, haptics, mitral valve, cardiac surgery.**

I. Problem Solved

A healthy mitral valve ensures the one-way flow of oxygenated blood from the left atrium to the left ventricle. Mitral regurgitation is a potentially serious condition in which oxygenated blood flows backwards across the valve, reducing cardiac efficiency and often necessitating surgical intervention.

While *repair* of the native valve tissue is recommended in nearly all cases, it is often avoided in lieu of simpler but less effective valve *replacement*, where native tissue is supplanted with a bio- or mechanical prosthetic. This results in significant increases in patient morbidities [1]. There is a strong correlation between repair rate and surgeon experience, with more experienced surgeons showing demonstrably higher rates of valve repair [2]. In the hope of increasing the repair rate, we have developed an interactive surgical simulation system for mitral valve repair to be used for training and patient-specific preoperative planning [3]. While others in the past have developed mechanical models of mitral valve, none operated at sufficient speeds to permit user interaction [4, 5].

II. Methods

A. Overview

3D medical images of the valve are segmented and processed to produce a patient-specific geometric and mechanical valve model. This model is then simultaneously rendered, computationally simulated, and modified by the user. This allows for the iterative testing of surgical modifications until a final surgical plan is developed (Figure 1).

A haptic interface greatly simplifies interaction with the 3D valve model. This requires a 1 kHz update rate to preserve haptic fidelity. Satisfying these user interaction requirements while maintaining simulation accuracy poses a major system design challenge.

This work was supported in part by the National Science Foundation Graduate Research Fellowship Program and the US National Institute of Health under grant NIH R01 HL073647-09.

N.A. Tenenholtz is with the Harvard School of Engineering and Applied Sciences. ntenenh@seas.harvard.edu

P.E. Hammer is with the Department of Cardiac Surgery, Children's Hospital Boston.

R.D. Howe is with the Harvard School of Engineering and Applied Sciences and the Harvard-MIT Division of Health Sciences and Technology.

B. Model Generation

We have developed an image processing pipeline that extracts mitral valve geometry from clinical 3D ultrasound volumes [6]. However, to isolate simulation error from geometric modeling error due to low ultrasound image quality, we use valve models derived from high-resolution microCT images of porcine valves in the development phase (Figure 2). Leaflet geometry and chordal connectivity are segmented and meshed from images of the unstressed, unpressurized valve. Displaced annular and papillary locations as well as chordal lengths are measured from closed valve images.

C. Simulation of Tissue Mechanics

While finite element models are the standard for mechanical membrane simulations, they are an order of magnitude slower than models based on mass-spring approximations. As shown by Hammer [5], these mass-spring models result in a minimal loss of accuracy for mitral leaflet tissue. Therefore, the system uses a bilinear mass-spring model of leaflet tissue with a critical strain of 25% to approximate a more complex Fung-elastic constitutive law (Figure 3). Chordae tendineae are treated as linear-elastic cylindrical rods with a 1 mm diameter supporting only uniaxial tension. Finally, Dirichlet boundary conditions are provided by the vertices located on the fibrous mitral annulus and papillary muscles.

D. Simulation of Pressurization

Simulation of dynamic blood flow in the heart is infeasible in a clinical planning system as it typically requires days of simulation time for each model. Therefore, we assess valve competency under a static peak-systolic pressure as this provides the greatest mechanical challenge to the valve and therefore the greatest potential for regurgitation. It also approximates a common intraoperative test for assessing valve competency.

E. Collision Handling

A penalty-based method is used to resolve self-collisions of the leaflet meshes during simulation. Potential collision pairs are first determined using a cache-friendly broad-phase sweep and prune algorithm, which exploits temporal coherence. A narrow-phase triangle-triangle collision detection algorithm assigns penalty forces on a node by node basis using a nonlinear, C^1 continuous, piecewise function.

F. Numerical Integration

Traditionally mass-spring meshes are integrated using an implicit scheme to guarantee stability [7]. However, this requires solving a large sparse linear system, typically through iterative methods. While this permits fast simulation to closure using large adaptive time steps, computing individual time steps can be costly. On the other hand, explicit integration methods simulate significantly smaller time steps at a much faster rate. For this interactive environment, explicit methods are more attractive as individual time steps must be simulated at fast haptic rates and the adaptive time stepping associated with implicit integration would have disoriented the user. This led to the use of a computationally efficient symplectic Euler integrator, which proved to be consistently stable with sufficiently small time steps.

III. Results

Geometric valve models were generated from images of three mitral valves taken from the freshly excised hearts of 30-40 kg female Yorkshire pigs. The face/vertex counts for the models were 655/414, 621/406, 624/425 respectively.

A. Simulation Accuracy

The three geometric valve models were simulated to closure and compared to the microCT images of the atrial surface of pressurized valves. The RMS error for the three valves, measured above leaflet coaptation, was 0.55 mm, 0.68 mm, and 0.66 mm, with maximum errors of 1.89 mm, 3.0 mm, and 2.2 mm respectively. Figure 4 shows a color map indicating the regions of greatest error on valve 3.

B. Simulation Speed

Simulation to valve closure took roughly 1 s on a desktop computer with a 2.67 GHz Intel Core i7-920 CPU and 6GB of RAM. Figure 5 shows the time profile of the simulation of valve 3. With the valve closed and pressurized, mean run time per time step across all three simulations was 453 µs. Greater than 99.99% of the time steps were simulated in less than the 1ms required for the 1 kHz haptic rate. These outliers were randomly distributed throughout the cardiac cycle and appear to be independent of valve state.

IV. Discussion

Simulation accuracy was overall very good, averaging 0.63 mm RMS. Error magnitude varied across valve geometry with the greatest errors occurring at the leaflet coaptation surface, which was caused by two primary factors. First, only the atrial surface of the microCT image is segmented due to the difficulty in separating coapted leaflets. In addition, after valve closure residual leaflet motion persists due to collision handling, making error vary with time. In the future, this will be mitigated by heavily over-damping the system upon valve closure.

Simulation speed also varied with valve geometry. As expected (and verified by code profiling), collision detection is the costliest operation thus explaining the performance profile in Figure 5. Peak performance is achieved in the leftmost region when the valve is unpressurized as there is minimal valve motion and no collisions. Performance decreases as the valve closes because large motions result in temporal incoherence, penalizing the broad-phase algorithm, and collisions begin to accumulate. Finally, upon valve closure, collisions occur in significant numbers burdening the narrow-phase algorithm, thereby reducing performance. Interestingly, as an ancillary benefit of explicit integration, the small time steps required for stability provide improved temporal coherence, thereby increasing the performance of the broad-phase algorithm throughout the simulation cycle.

The goal of this model was to simulate valve closure at haptic rates while preserving simulation fidelity. With 0.63 mm RMS simulation accuracy and a simulation rate of well over 2 kHz, these targets have been met. Moving forward, while preliminary investigations into surgical planning and post-surgical modification accuracy have been conducted [3, 5], further studies are necessary to demonstrate system efficacy.

[1] M. Enriquez-Sarano et al, "Valve repair improves the outcome of surgery for mitral regurgitation," *Circulation*, vol. 91, pp. 1022-1028, 1995.

[2] S. Bolling et al, "Predictors of mitral valve repair: clinical and surgical factors," *Annals of Thoracic Surgery*, vol. 90, no. 6, pp. 1904-1912, 2010.

[3] N. Tenenholtz, "On the design of an interactive, patient-specific surgical simulator for mitral valve repair," *2011 IEEE/RSJ International Conference on Intelligent Robots and Systems*, pp. 1327-1332, 2011.

[4] K. Kunzelman et al, "Fluid-structure interaction models of the mitral valve: function in normal and pathological states," *Phil. Trans. R. Soc. B*, vol. 362, no. 1484, pp. 1393-1406, 2007.

[5] P. Hammer, "Simulating heart valve mechanical behavior for planning surgical repair," Dissertation, Tufts University, 2011.

[6] R. Schneider et al, "Modeling mitral valve leaflets from Three-Dimensional Ultrasound," *Functional Imaging and Modeling of the Heart*, vol. 6666, pp. 215-222, 2011.

[7] D. Baraff et al, "Large steps in cloth simulation," *Computer Graphics*, pp. 43-54, 1998.

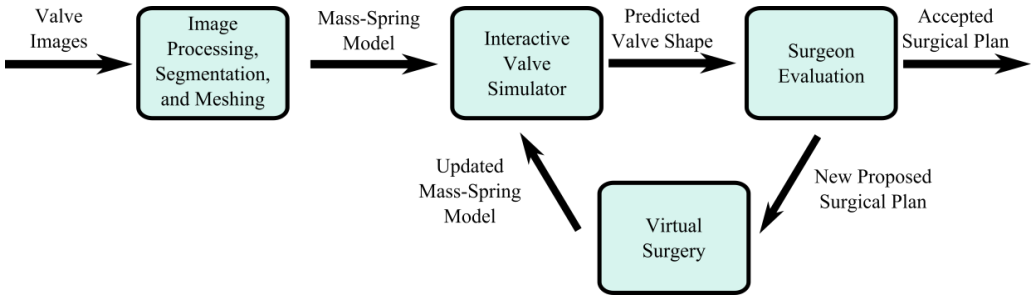

Figure 1: System workflow begins with model construction from 3D images, then an iterative process of simulation, surgeon evaluation, and virtual surgery until an acceptable procedure has been developed.

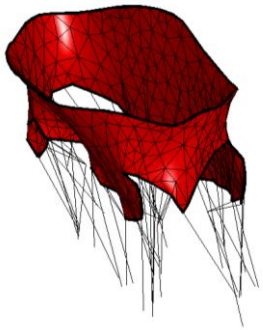

Figure 2: Valve model derived from the third porcine heart used for simulation.

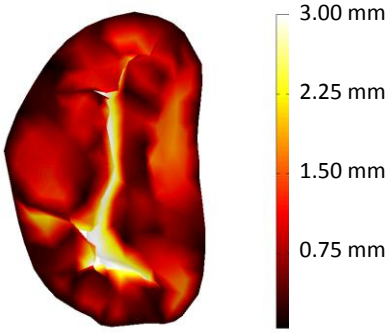

Figure 4: Simulation error for the third porcine heart simulated from the open state to closure. Color indicates error, defined as simulated leaflet distance from the leaflet shape in the experimental image of the closed valve.

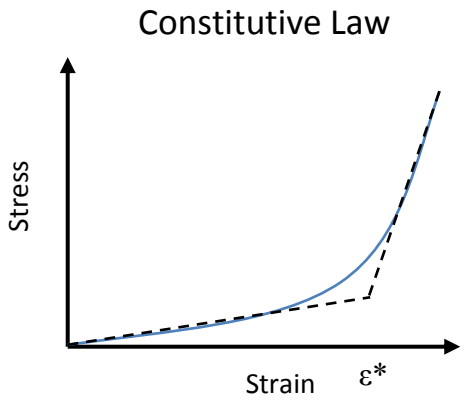

Figure 3: The nonlinear leaflet constitutive law (blue) is approximated by a bilinear function (dashed black) with a transition at critical strain ε* of 25% [???].

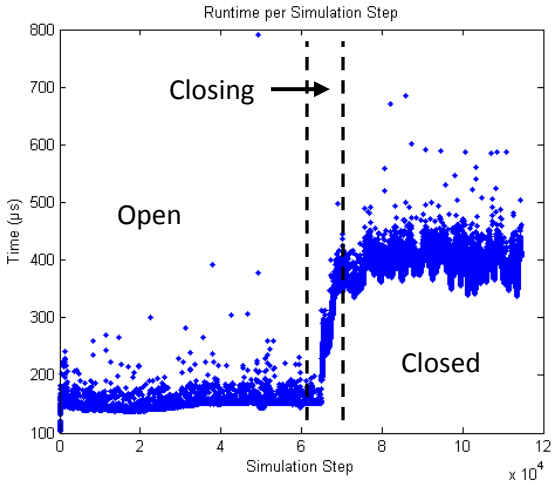

Figure 5: The runtime of each time step is plotted for a typical valve closure simulation. The increase during closure is largely due to collision handling.